Compounds co-targeting kinases in axon regulatory pathways promote regeneration and behavioral recovery after spinal cord injury in mice

Kar Men Mah[a,^], Wei Wu[b,^], Hassan Al-Ali[a,c,d], Yan Sun[b,e], Qi Han[b], Ying Ding[b], Melissa Muñoz[a], Xiao-Ming Xu[b], Vance P. Lemmon[a,d,f*], John L. Bixby[a,d,g*]

a. The Miami Project to Cure Paralysis, Dept of Neurological Surgery, University of Miami, Miami, FL, USA
b. Department of Neurological Surgery, and Stark Neurosciences Research Institute, Indiana University School of Medicine, Indianapolis, IN 46202
c. Peggy and Harold Katz Family Drug Discovery Center, Dept of Medicine, University of Miami, Miami, FL, USA
d. Sylvester Comprehensive Cancer Center, University of Miami, Miami, FL, USA
e. Department of Anatomy, Histology and Embryology, School of Basic Medical Sciences, Fudan University, Shanghai, 200032, China
f. Institute for Data Science and Computing, University of Miami, Miami, FL, USA
g. Dept of Molecular and Cellular Pharmacology, University of Miami, Miami, FL, USA

*Corresponding authors
^These authors contributed equally

Corresponding authors:
John L. Bixby, PhD
University of Miami Miller School of Medicine
1095 NW 14th Terrace, LPLC 4-17
Miami, FL-33136
Phone: 305-243-4874
Email: jbixby@med.miami.edu

Vance P. Lemmon, PhD
University of Miami Miller School of Medicine
1095 NW 14th Terrace, LPLC 4-16
Miami, FL-33136
Phone: 305-243-6793
Email: vlemmon@med.miami.edu

Highlights

- Kinase inhibitor RO48 targets both intrinsic and extrinsic axon-inhibitory pathways
- RO48 promotes neurite outgrowth in multiple neuronal types, including human neurons
- RO48 promotes corticospinal axon growth in injury models when delivered to cortex
- Axon growth induced by RO48 does not require an acute injury
- Results from distinct laboratories suggest that in vivo effects of RO48 are robust

Abstract

Recovery from spinal cord injury (SCI) and other central nervous system (CNS) trauma is hampered by limits on axonal regeneration in the CNS. Regeneration is restricted by the lack of neuron-intrinsic regenerative capacity and by the repressive microenvironment confronting damaged axons. To address this challenge, we have developed a therapeutic strategy that co-targets kinases involved in both extrinsic and intrinsic regulatory pathways. Prior work identified a kinase inhibitor (RO48) with advantageous polypharmacology (co-inhibition of targets

This is the author's manuscript of the article published in final edited form as:
Mah, K. M., Wu, W., Al-Ali, H., Sun, Y., Han, Q., Ding, Y., Muñoz, M., Xu, X.-M., Lemmon, V. P., & Bixby, J. L. (2022). Compounds co-targeting kinases in axon regulatory pathways promote regeneration and behavioral recovery after spinal cord injury in mice. Experimental Neurology, 114117. https://doi.org/10.1016/j.expneurol.2022.114117

including ROCK2 and S6K1), which promoted CNS axon growth *in vitro* and corticospinal tract (CST) sprouting in a mouse pyramidotomy model. We now show that RO48 promotes neurite growth from sensory neurons and a variety of CNS neurons *in vitro*, and promotes CST sprouting and/or regeneration in multiple mouse models of spinal cord injury. Notably, these *in vivo* effects of RO48 were seen in several independent experimental series performed in distinct laboratories at different times. Finally, in a cervical dorsal hemisection model, RO48 not only promoted growth of CST axons beyond the lesion, but also improved behavioral recovery in the rotarod, gridwalk, and pellet retrieval tasks. Our results provide strong evidence for RO48 as an effective compound to promote axon growth and regeneration. Further, they point to strategies for increasing robustness of interventions in pre-clinical models.

Keywords

kinase inhibitors, polypharmacology, axon growth, axon sprouting, pyramidotomy, pellet retrieval, reproducibility

Declaration of interest

HAA, VPL, and JLB are inventors on an international patent application filed by the University of Miami to cover the compounds described in this study (No. PCT/US18/58411).

Introduction

After traumatic injury, central nervous system (CNS) axons typically fail to regenerate, leading to irreversible loss of neuronal connectivity and associated functions. Regeneration failure can be attributed to both the axon-inhibitory environment of the injured CNS and the intrinsic inability of CNS neurons to mount a regenerative response following injury (Young, 2014). This poses a major hurdle for recovery from spinal cord injury (SCI) and other CNS injuries, such as traumatic brain injury and stroke (Huebner and Strittmatter, 2009). There are no drugs approved in the US for promoting CNS axon repair to aid functional recovery.

One obstacle challenging the translatability of candidate therapies for SCI has been the poor reproducibility of preclinical efficacy studies (Steward et al., 2012). Obstacles to reproducibility of published results include low "prior odds" of successful intervention, small effect sizes and small group sizes ("N's"), and lack of blinding and/or inappropriate allocation of animals to experimental groups (Bernard, 2020; Button et al., 2013; Ulrich and Miller, 2020; Watzlawick et al., 2019; Witt, 2019). The relative paucity of robust and reproducible effects in SCI studies may also be related to the observation that treatments targeting only one mechanism of axon regeneration are less effective (Lee et al., 2014). A promising paradigm in current drug development is the simultaneous engagement of multiple drug targets, termed polypharmacology (Al-Ali, 2016; Gray and Roth, 2006; Peters, 2013). Given that multiple mechanisms suppress axon growth in the CNS, polypharmacology is likely advantageous for SCI therapeutics, and perhaps even necessary (Al-Ali et al., 2016). Phenotypic screening campaigns, which implicitly accept polypharmacology, have been successful in delivering first-in-class drugs with novel molecular mechanisms of action (MoAs) (Eder et al., 2014; Swinney, 2013; Swinney and Anthony, 2011; Vincent et al., 2020). In fact, most current drugs appear to derive their efficacy and clinical success from having desirable polypharmacology with multiple MoAs (Al-Ali et al., 2016, 2015; Knight et al., 2010; Mestres et al., 2009; Metz and Hajduk, 2010; Peters, 2013; Petrelli, 2012).

We have focused our efforts on protein kinases, a versatile and highly tractable group of drug targets (Cohen, 2002). We screened over 1600 small molecule kinase inhibitors (KIs) in a hippocampal neurite outgrowth assay (Al-Ali et al., 2015, 2013). Using a platform called idTRAX (Identification of Drug TaRgets and Anti-targets by cellular and molecular Cross-referencing), we identified a pattern of polypharmacology that correlates with remarkable efficacy at promoting neurite outgrowth *in vitro,* and have identified a hit compound (RO480500-002; RO48) that exemplifies this pattern, by inhibiting multiple relevant kinase targets, including ROCKs (involved in extrinsic inhibition of axon growth) and S6K1 (implicated in intrinsic inhibition of axon growth) (Al-Ali et al., 2017, 2015; Gautam et al., 2019; Patel et al., 2020). We now demonstrate the ability of RO48 to promote neurite growth from a wide variety of neuronal types *in vitro*, and, more importantly, to promote corticospinal tract (CST) sprouting and/or regeneration in multiple mouse models of SCI. Notably, these *in vivo* effects of RO48 have been achieved in several independent experimental series performed in distinct laboratories at different times. Finally, in a dorsal hemisection model of SCI, RO48 not only promoted growth of CST axons beyond the lesion, but also led to significant behavioral recovery. Our data demonstrates the efficacy of RO48 as a compound that promotes CST growth and regeneration, and its robustness in multiple SCI models suggests its possible application as a therapeutic strategy for SCI and related neurological disorders.

Materials and Methods.

Viral particles. AAV8-UBC-TdTomato were generated at the Viral Vector Core of the University of Miami.

Cell culture. Primary rodent neurons were prepared and cultured as previously described for rat hippocampal neurons (Al-Ali et al., 2004), rat cortical neurons (Al-Ali et al., 2004), and mouse dorsal root ganglion (DRG) neurons (Lerch et al., 2017). For neuron-glia cocultures, hippocampal neurons were purified as before (Al-Ali et al., 2004) and seeded into plates containing astrocyte monolayer cultures, which were prepared as previously described (Beckerman et al., 2015). iPSC-derived glutamatergic neurons (ioGlutamatergic neurons, Bit.Bio)(Cambridge, U.K. Cat# E001) were prepared following the manufactures recommendations and plated in complete glutamatergic neuron medium: Neurobasal medium (Thermofisher (TF) 21103049), Glutamax (TF 35050061), 2-Mercaptoethanol (TF 31350010), B27 (TF 17504044), NT3 10 ng/ml (R&D 267-N3-025), BDNF 5ng/ml (R&D 248-BDB-005), doxycycline (Sigma D9891)). To avoid edge well effects, all cells were cultured in the inner 60 wells of 96-well plates, and edge wells were filled with PBS.

Neurite outgrowth assay. Neurons were seeded into PDL-coated 96-well plates (or those containing astrocyte monolayers), allowed to adhere for 24 hrs (human iPSC-derived glutamatergic neurons, 4000 cells/well) or 2 hrs (all other neurons), treated with compounds, then incubated for either 48 hrs (rat hippocampal neurons, rat cortical neurons), 16 hours (DRG neurons), or 24 hours (human iPSC-derived glutamatergic neurons). Plates were fixed, immunostained for β-III tubulin (Sigma-Aldrich T2200; 1:2000) and Hoechst 33342 10mg/mL(ThermoFisher Scientific H3570; 1:1000), then imaged in a Cellomics ArrayScan VTI high content analysis system as previously described (Al-Ali et al., 2004). Images were automatically traced using the Neuronal Profiling Bioapplication (Version 3.5). Raw data were managed by the Cellomics Store, which consists of an SQL database and a network-attached fileserver (HP). Data for all traced cells and the values for all the catalogued attributes (total neurite length, cell body shape, cell body size, nuclear intensity, etc) were exported from the SQL server in spreadsheet format. Subsequent data processing was automated in MATLAB. Several filters were applied to eliminate artifacts from entries using empirically determined cutoffs. For example, a minimum total neurite length of 10 μm was set for detected cells, to avoid inclusion of dead cells and debris when calculating total average neurite length. Additional filters include attributes for cell body size, number of neurite branches, and maximum neurite length without branches. After all filters were applied, the remaining objects constituted valid neurons. Processed data from valid neurons were finally analyzed to detect effects on neurite outgrowth, which was computed as neurite total length percentage of vehicle control (%NTL).

Animal Experiments. All experimental procedures including surgical interventions, behavior and electrophysiological assessments, and postoperative animal care were performed in accordance with the “Guide for the Care and Use of Laboratory Animals” (National Research Council), and were approved by the appropriate Institutional Animal Care and Use Committee (University of Miami or Indiana University School of Medicine). Animals were randomized in blocks and all animal experiments and analysis was conducted by individuals blinded to treatment conditions. Group sizes were determined by power analysis based on results from initial studies.

Unilateral Pyramidotomy. Adult C57BL/6J mice (8-10 weeks old) were anesthetized (100mg/kg Ketamine, 10mg/kg Xylazine IP). The head and ventral surface of the neck were shaved and wiped down with Nolvasan disinfectant solution. An incision was made 5mm lateral to the midline, underlying muscle were bluntly dissected to expose the surface of the ventrocaudal portion of the occipital bone. The caudal portion of the occipital bone was removed using laminectomy forceps to expose the right medullary pyramid. A feather microscalpel (15°, Electron Microscopy Sciences 72045-15) was used to puncture the dura and lesion the right

pyramidal tract (sham animals did not receive the lesion). Muscle was repositioned following the lesion and skin was closed using 4-0 Vicryl Sutures (Patterson Veterinary, 07-891-0083).

Cortical Microinjection. The head of the animal was placed on a stereotaxic frame. A midline incision was made to expose the skull and a craniotomy was performed over the left sensorimotor cortex. The compound and AAV8-UBC-TdTomato mixture (each 500 nl injection contained $1.25x10^{10}$ GC in PBS with 20% DMSO) was injected into five sites: -1.0mm anterioposterior (AP) and +1.0mm lateral, -0.25mm AP and +1.0mm lateral, +0.5mm AP and +1.5mm lateral, +1.25mm AP and +1.5mm lateral, +2.0mm AP and +1.5mm lateral (all coordinates in reference to bregma), at a depth of 0.5mm below the surface of the brain, using a pulled glass pipet connected to a nanoliter injector (WPI, Nanoliter 2010 with Micro 4 controller). After injection, the pipet was left in place for 1 minute before being withdrawn. The skin over the skull was pulled back and closed using 4-0 Vicryl Sutures.

Tissue processing and histology. Seven weeks after surgery, animals were anesthesized with an overdose of Ketamine/Xylazine and transcardially perfused with 4% paraformaldehyde. Tissues were left to fix overnight at 4°C in 4% paraformaldehyde before transferring to PBS the next day. The brainstem and cervical spinal cord were isolated and embedded in 2% agarose dissolved in PBS. 100μm sections were cut on a vibratome and mounted in Vectashield (with DAPI) (Vector Laboratories, H-1200-10), which were then imaged on an Olympus FV1000 confocal microscope. Completion of lesion to the pyramids were assessed by immunostaining spinal cord sections for PKC-gamma; sections were placed in Blocking solution (2.5% BSA, 0.01% Triton-X100 in PBS) for 1 hour at 4°C. Sections were then incubated overnight at 4°C in blocking solution containing PKC-gamma antibody (Abcam ab71558; diluted at 1:1000). The following day, sections were washed 3x in PBS and incubated in PBS containing secondary antibody (goat anti-rabbit Alexa 488) for 2 hours at room temperature with shaking. Tissue sections were then washed 5x in PBS and mounted in Vectashield (with DAPI) for imaging. To quantify the total number of labeled CST axons, axons were counted using the "Analyze Particle" plugin of FIJI (Schindelin et al., 2012). Axons were counted in five standard rectangular areas quasi-randomly placed in the pyramidal tract, and the calculated axon density was multiplied by the total area of the tract to obtain the total number of labeled axons. To count sprouted axons, three vertical dorso-ventral lines were drawn: adjacent, 400μm, and 800μm lateral to the central canal. The fibers crossing each line were counted by analyzing the peaks of the plot profile at the individual lines. The results were normalized to the number of labeled CST fibers: axon sprouting index is represented as the ratio of the total number of axons that cross the three lines described over the total number of labeled axons at the medulla. Five sections from C3-C5 were counted for each animal and averaged together. Experimenters were blinded to the treatment groups at all steps.

Dorsal hemisection and funiculotomy. Female C57BL/6 mice (7 weeks, Charles River, Wilmington, MA), were housed in groups under a constant 12 h dark/light cycle with food and water supplied. We chose female over male mice because the urinary bladder voiding in female mice can be better managed, and no difference was found in functional and histological outcomes after a contusive SCI in age-matched rodents in our recent study (Walker et al., 2019).

Surgical procedures. After 3 weeks behavioral training and baseline assessments, mice were anesthetized with a cocktail of ketamine/xylazine (120 mg/kg; 3.3 mg/kg). Following a cervical midline skin incision, transverse processes of C5/6 vertebra were stabilized (Zhang et al., 2013). A durotomy at the interlaminar space between C5 and C6 was performed using a 30G needle followed by a pair of microscissors. The dorsal hemisection was created by using a VibraKnife attached to the Louisville Injury System Apparatus (LISA, Louisville Impactor System, Louisville,

KY) (Al-Ali et al., 2017), which can produce the cutting accuracy at 0.01 mm (Zhang et al., 2013). The blade was advanced 1.2 mm (dorsal hemisection) or 0.9 mm (funiculotomy) ventrally from the dorsal surface of the spinal cord, extending beyond the central canal to make sure that the dorsal and lateral corticospinal tracts were completely transected. This is critical for assessing forelimb dexterous and general locomotor function. After the injury, the mouse head was fixed firmly onto a head holder (SG-4N, NARISHIGE, Amityville, NY). A craniotomy was performed followed by stereotaxic injections of treatment compounds into the sensorimotor cortex on each side (coordination: anteroposterior/mediolateral to the bregma 2 mm/1.5 mm, 1.25 mm/1.5 mm, 0.5 mm/1.5 mm, -0.25 mm/1 mm, and -1 mm/1 mm; depth: 0.5 mm) with 1 µl/injection. Animals were assigned into four groups (blindly labeled with A, B, C, D) that received cortical injections of compound or vehicle solution. After surgery, animals were returned to their home cages and received appropriate post-surgery care.

Forelimb behavioral tests. Behavior experiments were conducted in a randomized and blinded fashion. Animals were randomized into groups and treated with letter-coded reagents. Experimenters were blinded to the identity of treatments during the behavioral tests. Upon completion of the experiments, mouse groups were analyzed and then decoded. The grid walking test was employed to assess the sensorimotor coordination and precise stepping control of forelimbs. The test was performed according to a previously established protocol (Al-Ali et al., 2017; Wu et al., 2017). Briefly, animals were placed on a wire grid (10 x 10 mm^2) for walking training for 3 days before experiments. The percentage of forepaw drops below the grid plane during a 3 min observation period was calculated at 3 d before injury (as a baseline) and at 1, 2, 4, 6 and 8 weeks after the C5 dorsal hemisection (C5-DH). Single-pellet retrieval test is a standard assessment for forelimb dexterous function. This test was performed and modified according to our previously published work (Al-Ali et al., 2017). Briefly, mice were pretrained to use their forelimb to grasp and retrieve food for 2 weeks till the success rate reached at around 50%. During this period, a preferred forelimb was decided for each animal. Because all animals were provided with limited amount of food (10% - 20% of body weight) 2 days before tests and fasting for 12 hours before conducting the pellet-retrieval assessment, any mouse whose weight dropped more than 10% of the baseline bodyweight was excluded from the study. The test was conducted in a separate quiet room to minimize the environmental perturbation that might lead to distraction and inadequate food-retrieving movement. Four parameters, including fail to touch, touch, fail to retrieve, and retrieve, were used to assess dexterous forelimb function after SCI. Percentage of each parameter was calculated by dividing the number of the attempts of a particular parameter by the sum of all attempts. Statistical analysis was done using two-way ANOVA with Tukey's post hoc test. The Rotarod test was used to assess motor coordination in rodent, in accordance with previously described method (Liu et al., 2013). Briefly, mice were placed on a rotating rod (diameter 30 mm) on a Rotarod device (IITC Life Science, Woodland Hills, CA) that accelerated from 0-30 rpm within a 90-second period. The total testing duration was 120 seconds per animal, and the times when each mouse fell from the rotating bar was recorded. The rotarod test was performed at the predetermined experimental timepoints.

Anterograde tracing and immunofluorescent staining. Biotinylated-dextran amine (BDA, 10,000 MW, 10% in saline, Invitrogen) anterograde tracing was performed at 8 weeks after the dorsal hemisection. Mice received bilateral injections of BDA into the sensorimotor cortex to trace the CST axons anterogradely. Five stereotaxic injections of BDA (0.5 µl/each site) on each side were made using the same coordinates as the RO48 injections described above. The injection speed was 0.1 µl/min using the Stoelting motorized integrated stereotaxic injectors system

(Stoelting, Wood Dale, IL). CST axons were visualized by immunofluorescent labeling of BDA in the spinal cord according to our previously published protocol (Wang et al., 2014). Mice were sacrificed by giving a lethal dose of anesthesia and perfused with phosphate buffered saline (PBS) and 4% paraformaldehyde (PFA). Spinal cords were harvested and dehydrated via increasing concentrations of sucrose (up to 30%). The spinal cords were sectioned sagittally at 25 µm (dorsal hemisection) or 30 µm (funiculotomy) thickness. The lesion was defined by immunofluorescent labeling of glia fibrillary acidic protein (GFAP; 1:1000, AB5804, Chemicon, Temecular, CA). BDA-labeled CST axons were stained using avidin-biotin peroxidase incubation, followed by standard amplification with tyramide (SAT7000, PerkinElmer, Waltham, MA). Three sagittal sections of each spinal cord spaced 300µm apart were chosen for analysis. The middle section was defined as the one that cut through the central canal, and the other two are 150µm lateral to the midline section to either the right or the left side. The number of BDA-labeled CST axon fragments was counted at defined zones spaced 0.2 mm apart (dorsal hemisection) or 0.1 mm apart (funiculotomy). The axon number was standardized into CST Axon Index defined as ratio of the BDA-labeled axon number at a given zone over the total number of axons in the descending CST on a cross section of the C1 spinal cord. The lesion epicenter on the sagittal section is defined as "0" and all other zones are defined as their distance from the lesion epicenter.

Results

RO48 promotes growth of multiple neuronal types in vitro. RO48 was initially identified as a strong promoter of neurite outgrowth using embryonic hippocampal neurons (Al-Ali et al., 2015; **Fig. 1a**). We previously found, however, that KIs promoting neurite outgrowth in certain neuronal types may have weak or no outgrowth-promoting activity in others (Al-Ali et al., 2004). To examine this issue for RO48, we tested it in additional neuronal models, including postnatal cortical neurons (**Fig. 1b**) and adult sensory neurons (**Fig. 1c**); RO48 consistently promoted neurite outgrowth in each of these cell types. RO48 also promoted neurite growth in cortical neurons grown on an inhibitory glial substrate (Fig. 1d), consistent with its ability to interfere with neurite-inhibitory signaling through ROCK. To examine whether RO48's activity extended to human neurons, we tested it using human iPSC-derived glutamatergic neurons (**Fig. 1e, f**). RO48 strongly promoted neurite growth in these neurons, suggesting that its molecular mechanism of action (MoA) is conserved across a range of neuronal types (and species), and therefore that it might promote axon regrowth in a variety of *in vivo* contexts relevant to regeneration.

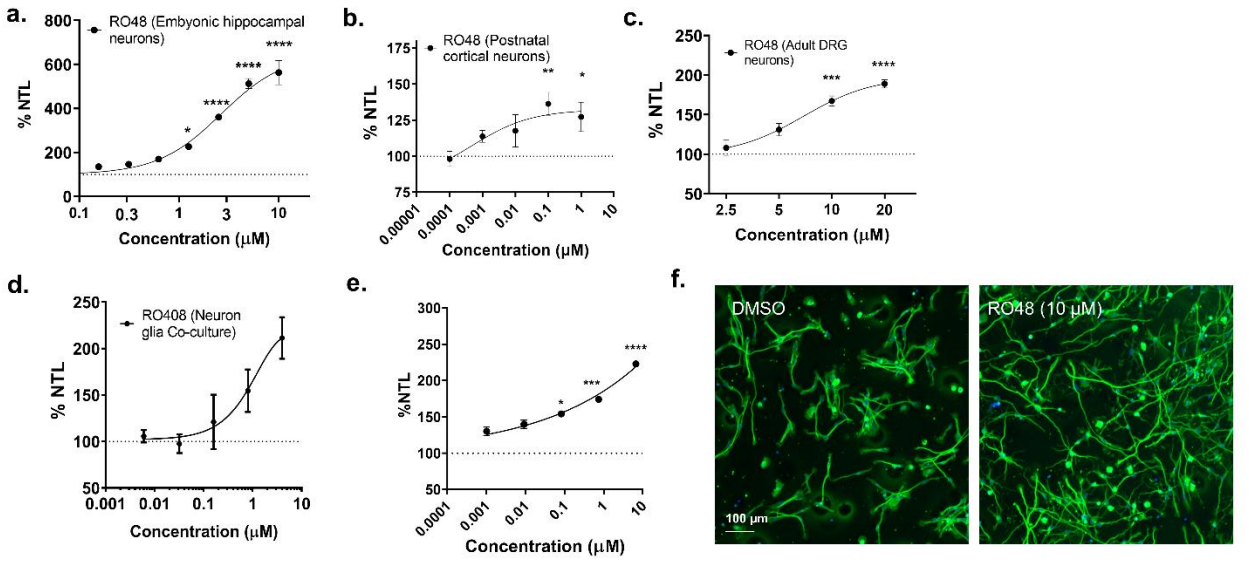

Figure 1. **RO48 promotes neurite outgrowth in a variety of mammalian neurons.** RO48 strongly promotes neurite outgrowth in a variety of neurons including a) rat embryonic hippocampal neurons, b) mouse postnatal cortical neurons, c) mouse adult dorsal root ganglion (DRG) neurons, d) neuron-glia co-culture, and e) human iPSC-derived glutamatergic neurons. f) Representative images of iPSC-derived glutamatergic neurons treated with RO48 or DMSO vehicle for 24 hours and immunostained for βIII-tubulin (green, cell bodies and neurites) and nuclei (blue, Hoechst). Images were acquired using a Cellomics VTI microscope. Co-culture: Mean ± SD, all other data: Mean ± SEM, n ≥ 3. One-way ANOVA with Dunnet's multiple comparison's test (*p<0.05, ***p<0.001, ****p<0.0001).

RO48 cortical microinjection promotes sprouting of CST axons in the cervical spinal cord after unilateral pyramidotomy. Earlier, we tested RO48 in a mouse unilateral pyramidotomy model, and found that infusing the compound into the CSF (over 28 days) doubled the amount of axonal sprouting by contralateral corticospinal tract (CST) axons in the cervical cord (Al-Ali et al., 2015). In the current experiments, we altered the experimental setup in two important ways. First, we delivered RO48 by direct injection into sensorimotor cortex, which allowed a) the use of a smaller dose (5 µL of 1 mM solution, corresponding to ~0.125 mg/kg), and b) more precise targeting of the compound to the neurons of origin of the uninjured CST. We have successfully used cortical microinjection as a way to deliver other KIs to these neurons in the past (Al-Ali et al., 2017; Wang et al., 2014). We found that cortical microinjection of RO48 allowed it to reach targets in the brain, as it decreased pS6 (a measure of S6K1 activity) in brain tissue in a dose-dependent manner (**Fig. 2c**). Second, to test whether RO48 can promote axon sprouting without acute denervation, we added experimental groups that received RO48 (or vehicle) but did not experience pyramidotomy. Following pyramidotomy, RO48 increased contralateral sprouting when delivered by cortical microinjection; in this case by roughly 3-fold over control (0.067 (95% CI 0.054, 0.080) vs 0.024 (95% CI 0.013, 0.40); **Fig. 2a,b**). Interestingly, RO48 also increased axonal sprouting in animals without pyramidotomy, with a similar fold increase compared to uninjured vehicle-treated animals (**Fig. 2a,b**; 0.046 (95% CI 0.040, 0.055) vs 0.017 (95% CI 0.011, 0.023)). These data suggest that RO48 can exert its effects on contralateral sprouting without requiring "priming" cues from a recent injury event.

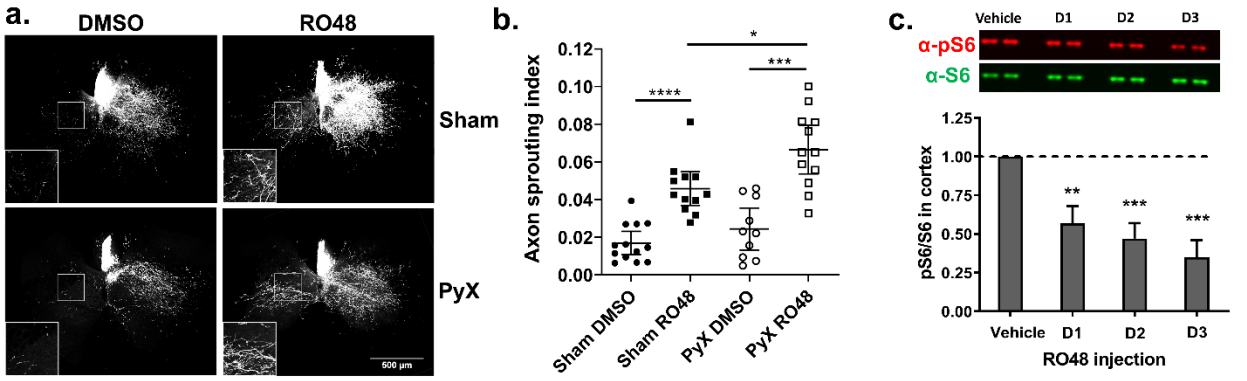

Figure 2. RO48 injection into sensorimotor cortex promotes axon sprouting. a) Transverse sections of cervical spinal cord 7 weeks after unilateral pyramidotomy (PyX) or sham surgeries and co-injection of AAV8-GFP and test compounds into the sensorimotor cortex show increased contralateral axon sprouting in animals treated with RO48 for both Sham and PyX. Insets show increased magnification of boxes highlighted in the approximate equivalent region in respective panels. b) Quantification of contralateral axon sprouting index in animals injected with RO48 (2.5 µL of 2 mM solution, corresponding to ~0.125 mg/kg) or DMSO. Graph represents one data point per animal, mean, and 95% CI of sprouting index for animals with or without pyramidotomy (N=12/group). One-way ANOVA with Bonferroni post-test, *p < 0.05, ***p < 0.001. c) Top: Western blot of brain homogenate collected 1hr after injection of RO48 (2 animals/condition/experiment). Bottom: Densitometric quantification of Western blot of pS6 levels relative to pan S6. Data normalized to vehicle (DMSO) control. Mean ± SEM, n=3 experiments with two animals per dose (D1, D2, D3) per experiment. D1= 1.2 µL of 1 mM solution, corresponding to ~0.03 mg/kg; D2= 1.2 µL of 10 mM solution, corresponding to ~0.3 mg/kg; D3= 1.2 µL of 100 mM solution, corresponding to ~3 mg/kg. One-way ANOVA with Tukey post-test, **p < 0.01, ***p < 0.001.

RO48 cortical microinjection 8 weeks post injury promotes CST axon sprouting in the spinal cord in a unilateral pyramidotomy model. The previous experiments suggest investigation of the efficacy of RO48 in a chronic injury experimental paradigm. We tested if RO48, when microinjected into the sensorimotor cortex 8 weeks following unilateral pyramidotomy, could promote sprouting of uninjured CST axons into the denervated contralateral cervical spinal cord. In this experiment, animals first receive a pyramidotomy, and were allowed to recover for 8 weeks. The animals then underwent a second procedure in which RO48 or DMSO were co-injected with the AAV8-TdTomato tracer to label uninjured CST axons. Animals were sacrificed 5 weeks after microinjections and the axon sprouting in the cervical spinal cord was assessed (see **Fig. 3a** for timeline). Though the animals received microinjections at a delayed timepoint, animals that received RO48 exhibited increased axonal sprouting, about a 3-fold increase compared to control animals (**Fig. 3b,c**; 0.549 (95% CI 0.418, 0.680) vs 0.178 (95%CI 0.119, 0.237)). These data indicate that RO48 can promote axon sprouting even when administered weeks after injury, and suggest possible application in clinical settings where immediate therapeutic treatment after an injury may not be feasible.

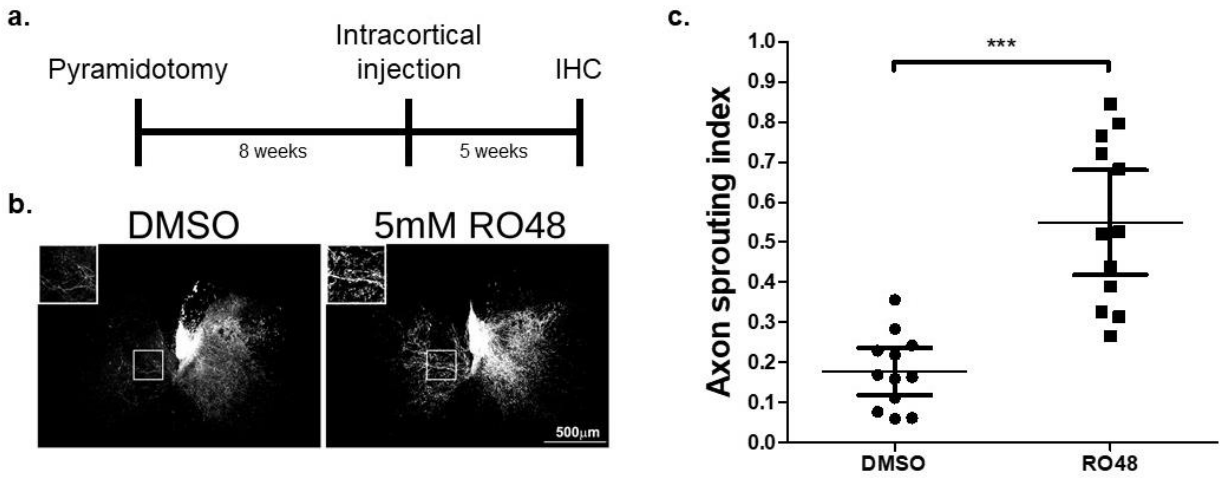

Figure 3. RO48 injection 8 weeks after pyramidotomy promotes axon sprouting. a) A schematic of the experimental timeline with procedures and assessment. IHC; immunohistochemistry. b) Transverse sections of cervical spinal cord 5 weeks after injection of AAV8-TdTomato and 5mM RO48/DMSO into the sensorimotor cortex show increased contralateral axon sprouting in animals treated with RO48 8 weeks after pyramidotomy. Insets show increased magnification of boxes highlighted in the approximate equivalent region in respective panels. c) Quantification of contralateral axon sprouting index in animals injected with RO48 (2.5 µL of 5 mM solution) or DMSO. Graph represents one data point per animal, mean, and 95% CI of sprouting index for animals (N=12/group). Student's T-test, ***$p < 0.001$.

RO48 cortical microinjection promotes CST axon growth in the spinal cord in a cervical funiculotomy model. The pyramidotomy experiments showed that cortical microinjection of RO48 can promote axon growth in CST target regions. We previously demonstrated that microinjection of other KIs, targeting PKC and S6K1 respectively, can promote regeneration of injured CST axons after a spinal cord injury (Al-Ali et al., 2017; Wang et al., 2014). As an initial test of RO48's ability to promote regeneration of the injured CST, we performed a C5 dorsal funiculotomy to sever the dorsal CST (dCST) in mice, performed cortical microinjections with RO48 or DMSO vehicle, and examined growth of CST axons in the cervical cord at 8 weeks post injury (wpi). We found that RO48 treatment promoted extensive growth of the CST axons, anterogradely labeled by BDA, across and beyond the lesion site (**Fig. 4**). In RO48-treated animals (but not controls), we saw strong sprouting of CST axons in the gray matter proximal to the injury, and labeled axons could also be seen traversing the injury site and growing caudally for several mm (**Fig. 4a,b**). The numbers of sprouting axons in the gray matter rostral to the injury were about 5 times higher than controls, and numbers of axonal processes caudal to the injury were more than 10 times higher than in control animals, up to 2-3 mm beyond the injury (**Fig. 4c**). Axon growth caudal to the injury and sprouting proximal to the injury could be found in each animal receiving treatment with RO48. These data suggest that RO48 can promote regrowth of injured CST axons in the spinal cord.

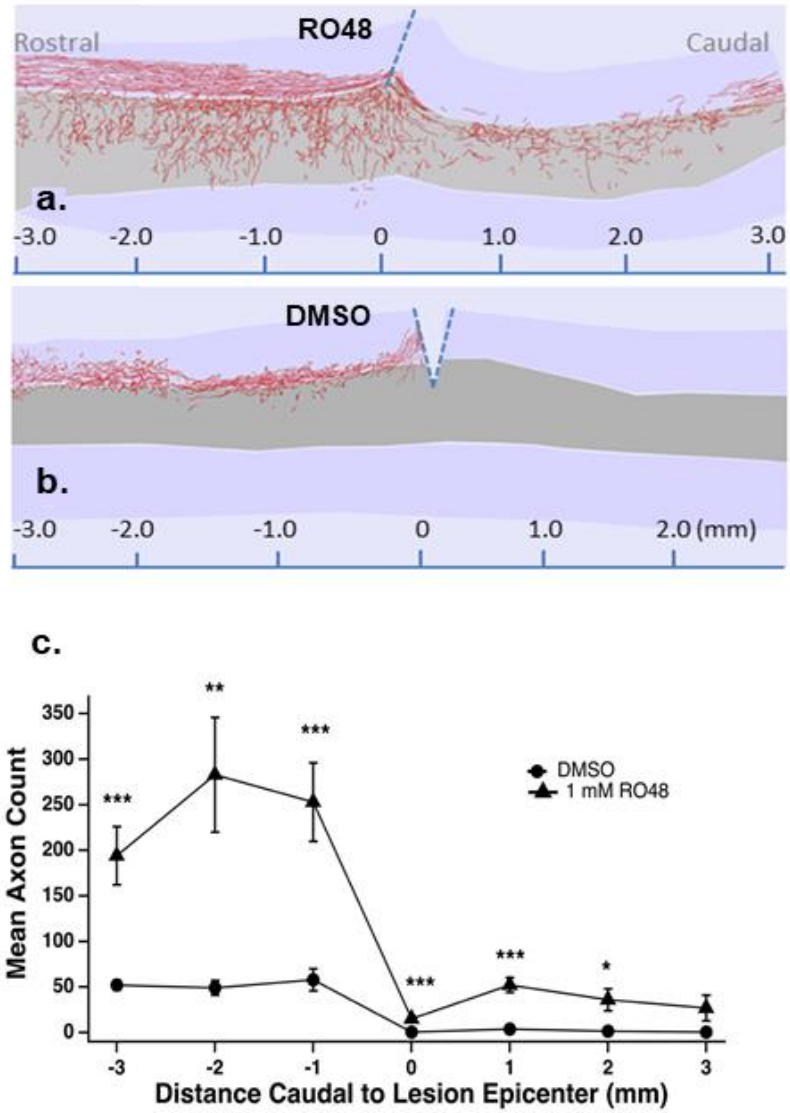

Figure 4. Direct microinjection of RO48 promotes sprouting and regeneration of the corticospinal tract (CST) after dorsal funiculotomy. (a, b). Representative sagittal sections of cervical spinal cord from injured animals that underwent funiculotomy injury followed by cortical microinjection of either (a) RO48 (10 µL of 1 mM, corresponding to ~0.25 mg/kg) or (b) DMSO vehicle. CST fibers labeled by BDA injection into sensorimotor cortex are traced in red; area of transection injury is indicated by blue dotted lines. Spinal cord gray matter is colored gray; white matter is purple. Rostral is to the left in each image. Longitudinal distance scale on the x axis is indicated in mm; the epicenter of the lesion is indicated as 0. (c). Quantitative estimates of CST growth rostral and caudal to the hemisection injury. Axons were counted from transverse sections crossing lines at each distance indicated from lesion epicenter. Three sections were counted for each animal; the total number of axons per section at each distance for each animal was averaged. N = 6 animals, RO48; N = 5 animals, DMSO. Means and SEMs are plotted. *, $p < 0.05$; **, $p < 0.01$; ***, $p < 0.005$, t-test.

RO48 promotes axon growth and behavioral recovery in a cervical dorsal hemisection model. To increase confidence in the ability of RO48 to promote growth of injured CST axons, and as a

check on robustness, we turned to a dorsal hemisection model, which transects both the dCST and the dorsolateral CST (dlCST), eliminating labeled CST axons distal to the C5 injury in controls ((Al-Ali et al., 2017); **Fig. 5a**). In these experiments, we used two doses of RO48 (1mM; RO_1; and 5mM; RO_5) and compared these to DMSO control and to Y27632 (1mM), an inhibitor of ROCKs and other kinases which has been shown to promote axon regeneration and behavioral recovery after spinal cord and optic nerve injury (Chan et al., 2005; Fournier et al., 2003; Ichikawa et al., 2008; Lingor et al., 2008). In sagittal sections from vehicle-treated animals taken 8 wpi, BDA-labeled CST axons were sparse in the gray matter immediately rostral to the injury site, and essentially no axons were detected caudal to the injury. In both RO48-treated animals and Y27632-treated animals, CST sprouts could be detected in the gray matter rostral to the injury site, and labeled axons could clearly be seen caudal to the injury. These labeled CST axons appeared denser in RO48-treated animals than in those treated with Y27632 (**Fig. 5b,c,d**). Quantitative analysis of labeled CST axons confirmed that treatment with Y27632 and with RO48 at 1 mM resulted in less CST axon dieback proximal to the lesion (compared to control), and that treatment with RO48 at 5 mM resulted in decreased axon dieback as well as increased axon growth distal to the lesion, compared both to the DMSO control and to Y27632 (**Fig. 5e**).

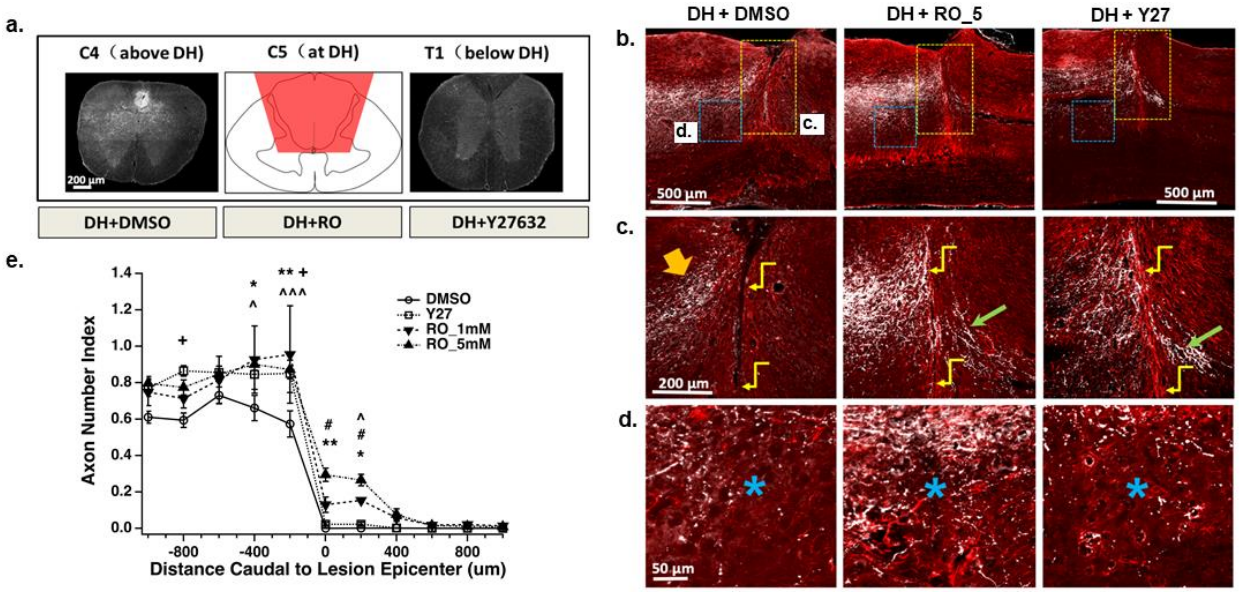

Figure 5. Direct microinjection of RO48 promotes sprouting and regeneration of the corticospinal tract (CST) after cervical dorsal hemisection. a) Animals received a C5 dorsal hemisection injury with a Vibraknife (red area in drawing of transverse section in middle panel), followed by microinjection of Y27632 (10 µL of 1mM, corresponding to ~0.16 mg/kg, Y27), low dose of RO48 (10 µL of 1mM, corresponding to ~0.25 mg/kg, RO_1), high dose of RO48 (10 µL of 5mM, corresponding to ~1.25 mg/kg, RO_5), or DMSO. Transverse section of control animal at C4 (left) shows BDA-labeled CST axons (white), while a similar section at T1 (right panel) shows that axons were not detectable below the lesion in control animals. b-d) Sagittal sections showing lesion areas from (left) control, (center) RO48-treated, and (right) Y27632-treated animals. Boxes in b) panels show areas enlarged in c) yellow and d) blue. Green arrows in c) show regenerating fibers in RO48- and Y27632-treated animals, angled yellow arrows mark lesion site, and thick gold arrow in left panel shows dCST. Asterisks in d) show areas of gray matter sprouting rostral to the injury, which is increased with RO48 treatment. e) Quantification of CST axons at different distances from the lesion site, measured as Axon Number Index.

Axonal dieback is reduced, and growth beyond the lesion is increased, by Y27632, and more so by RO48 at 1 mM and at 5 mM. **p< 0.01, *p<0.05, RO 5mM vs. DMSO; #p <0.05, RO 5mM vs. Y27632; ^^^p< 0.001, ^p< 0.05, RO 1mM vs. DMSO; +p< 0.05, Y27632 vs. DMSO.

Because regenerative responses after experimental treatments need not correlate with improvements in behavioral recovery (Wang et al., 2015), we incorporated forelimb behavioral outcome measures in this set of experiments. Cervical spinal cord injuries lead to measurable functional deficits including in forelimb and hindlimb motor coordination, balance, forelimb motor and proprioceptive function, and precise and coordinated forelimb movements (Anderson et al., 2005; Forgione et al., 2017; Schrimsher and Reier, 1992; Streijger et al., 2013) . To test these functions, our outcome measures included gridwalk (forepaw drop error), rotarod, forepaw adhesive tape removal, and pellet retrieval tests (Al-Ali et al., 2017; Liu et al., 2013). Significant improvements in recovery were seen in RO48-treated animals compared to vehicle controls in the gridwalk, rotarod, and to a slight and variable extent in the pellet retrieval assay, and for Y27632-treated animals in gridwalk and rotarod (**Fig. 6**). Overall, these data suggest that a single cortical injection of RO48 can improve motor outcomes after a dorsal hemisection injury to the spinal cord. Note that Y27632 promoted axon growth in our injury model, and slightly improved functional outcomes, consistent with previous reports (Chan et al., 2005; Fournier et al., 2003; Ichikawa et al., 2008; Lingor et al., 2008), though it was not as effective as RO48. Presumably, differences among experiments in the extent of regeneration and/or functional recovery induced by Y27632 are due to differences in injury models and/or the route of compound delivery, as well as unknown factors.

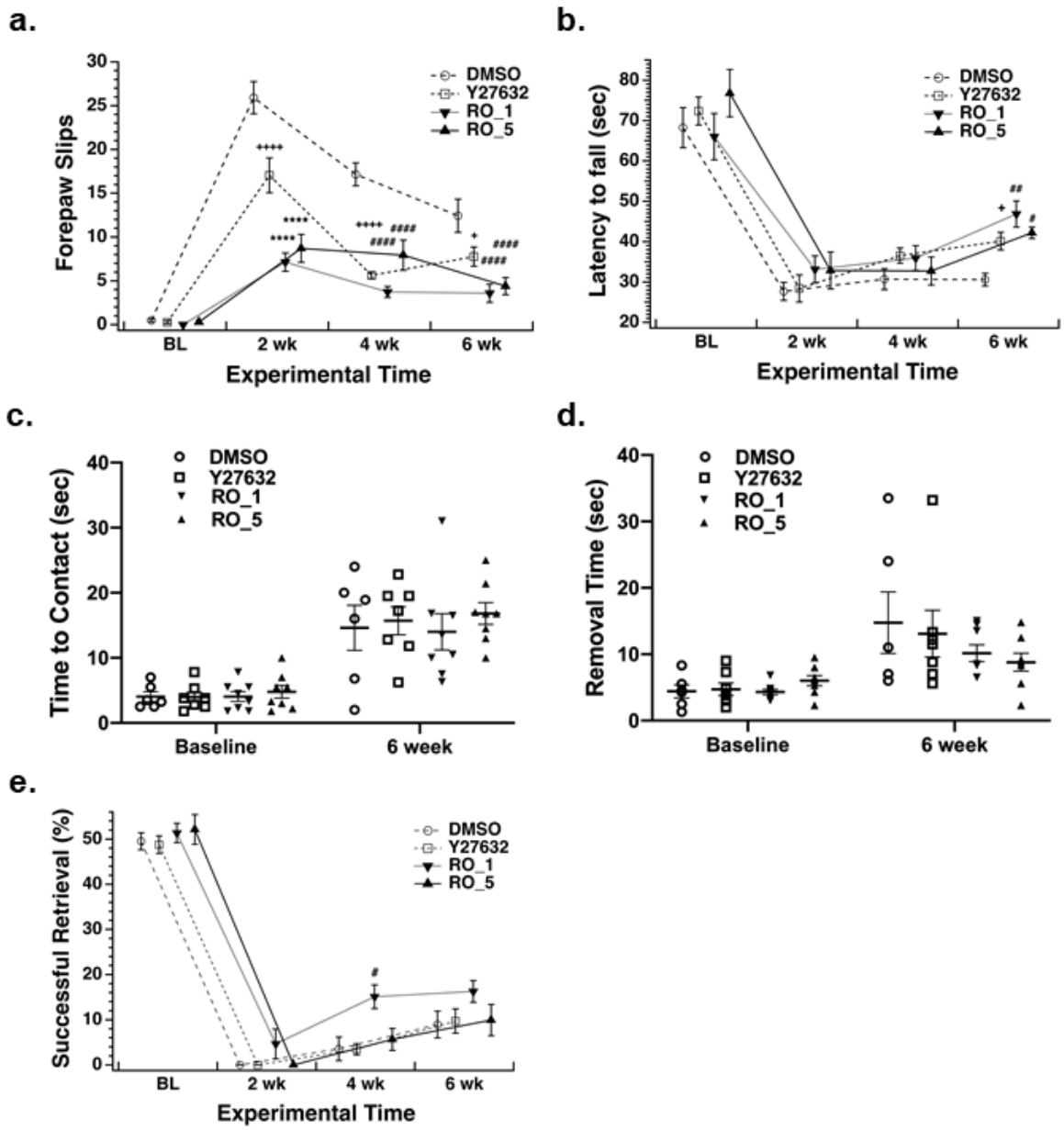

Figure 6. Cortical microinjection of RO48 and Y27632 improves behavioral recovery after hemisection injury. a) Number of forepaw slips below the grid in gridwalk test is plotted for DMSO (control, open circles), Y27632 (open squares), low dose of RO48 (RO_1, downward triangles) and high dose of RO48 (RO_5, upward triangles). Slips were rare in all groups at baseline. By 2 weeks post injury (wpi), forepaw slips were fewer in both RO48 groups compared to DMSO control and to Y27632. Gradual improvements were seen in the DMSO group at 4 and 6 wpi, but improvements were significantly more rapid and extensive in both RO48 groups and in the Y27632 group. b) Latency to fall from rotarod. All groups were able to stay on the rod for about 70 sec at baseline, and did more poorly when tested at 2 wpi. By 6 wpi, both RO48 groups and the Y27632 group were able to remain significantly longer than DMSO controls. c, d) Results from adhesive test. c) No differences were seen among groups in the time that animals took to sense and contact the adhesive strip. d) At 6 wpi, animals in the RO48 groups appeared to remove the adhesive more rapidly, but these differences did not reach statistical

significance. e) After training in the pellet retrieval test, each group reached retrieval success rates close to 50%; these rates fell substantially in all groups when tested at 2 wpi. None of the groups achieved high success rates by 6 wpi, though the RO48 low group appeared better at 4 and 6 wpi than the other three groups, and this difference was statistically significant from DMSO at 6 wpi. Symbols for data of the different groups collected at the same time point are offset on the x axis for clearer visualization. Data are expressed as mean ± SEM ,n=8; ****p < 0.0001, **p < 0.01, RO_1, RO_5 vs Y27632, DMSO; ++++p < 0.0001, +p < 0.05, Y27632 vs DMSO; ####p < 0.001, ##p < 0.01, #p < 0.05, RO_1, RO_5 vs DMSO.

RO48 promotes CST regeneration and forelimb functional recovery after a C5 cervical dorsal hemisection. The funiculotomy and initial dorsal hemisection experiments suggest that RO48, when delivered to the cortical neurons that form the CST, can promote sprouting and regeneration of CST axons in the spinal cord, and can improve behavioral recovery after injury to the dorsal cervical cord. We attempted to validate these findings by repeating the dorsal hemisection injury, testing higher doses of RO48 (4mM; RO_4; and 30mM; RO_30) in hopes of more consistent behavioral recovery. In addition to the negative control group (DMSO vehicle), we included a group treated with injection of the S6K1 inhibitor PF-4708671 (PF) (10mM); this is the highest dose that we have previously shown to produce CST regeneration and improve behavioral recovery after a dorsal hemisection (Al-Ali et al., 2017). The timeline for these experiments is shown in **Fig. 7a**. The BDA tracer was cortically injected at 8 wpi (**Fig. 7b**), prior to examination of the labeled axons at 10 wpi, as previously detailed (Al-Ali et al., 2017). In both DMSO and PF treatment groups, the labeled CST main tract stopped at the rostral lesion border (**Fig. 7c, d, g, h**). In striking contrast, both 4mM and 30mM RO48 treatment groups exhibited numerous BDA-labeled CST axons regenerating through and beyond the lesion gap and elongating within the gray matter of the distal spinal cord (**Fig. 7e, f, i, j**). Quantification of CST axons showed that both RO48 treatments significantly enhanced CST axonal sprouting (or prevention of die-back) rostral to the lesion site compared to the PF and DMSO groups, and notably, only in the RO48 groups were CST axons found to traverse and grow beyond the lesion site (**Fig. 7k, l**). No significant differences were observed between the two RO48 treatment groups. These results confirm that RO48 consistently promotes sprouting and regeneration of injured CST axons. It is interesting that PF did not promote axon growth above control levels seen in these experiments, since it significantly promoted growth in previous experiments (Al-Ali et al., 2017). This discrepancy may be due to our observation that the lesion depths in the current experiments were greater than in previous animals (1.2mm as compared to 0.9mm; completed by a different surgeon for the 2017 study), leading to a more severe injury. This points up the challenge of replicating spinal cord injury experiments, but at the same time suggests that the effects of RO48 may be unusually robust.

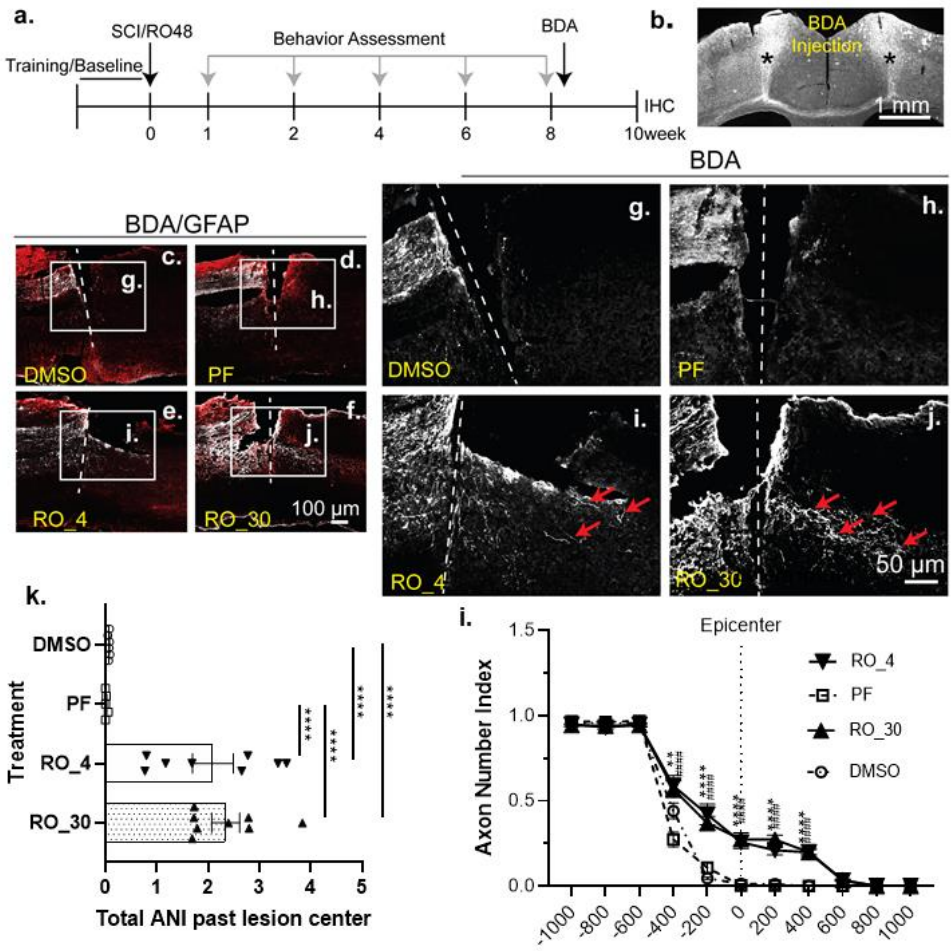

Figure 7. RO48 injected into sensorimotor cortex promotes long distance axon growth after C5 dorsal hemisection. a) Timeline, procedures and assessments. b) Coronal section of cortex showing bilateral injections of BDA; injection sites indicated by asterisks. (c-f) Representative sagittal sections (dotted line indicating injury epicenter) show BDA-labeled CST axonal terminals at or beyond the lesion gap (defined by GFAP labeling, red) in animals that received DMSO (control, c), PF (10 µL of 10 mM, corresponding to ~2 mg/kg, d), low dose RO48 (10 µL of 4 mM, corresponding to ~1 mg/kg, RO_4; e), or high dose RO48 (10 µL of 30 mM, corresponding to ~7.5 mg/kg, RO_30; f). g-j) Magnifications of boxed areas in c-f show that BDA-labeled CST axons regenerated across the lesion gap (dashed line) and extended within the distal spinal cord only in RO48 groups (red arrows in i,j). k,l) Quantitative analysis of labeled CST axons at different distances from the lesion site; number of axons counted at indicated distances is normalized as axon number index (ANI). k) The ANI surrounding the lesion epicenter is summed and graphed as mean ± SEM. Both high and low doses of RO48 greatly enhanced CST axonal regeneration beyond the lesion gap compared to DMSO- and PF-treated groups. **l**) Comparison of the ANI at 200 µm spaced distances rostral and caudal to the lesion gap. Data are expressed as mean ± SEM. n=6-8/group. ***p<0.001, ****p<0.0001, RO_30 vs DMSO two-way ANOVA followed by Tukey's post hoc test; ####<0.0001 RO_30 vs PF, two-way ANOVA followed by Tukey's post hoc test.

To confirm the effects of RO48 on behavioral recovery, we again performed longitudinal tests of forelimb function, including rotarod, gridwalk, and pellet retrieval (**Fig. 8**). In the rotarod test, we measured latency to fall. Before injury, no significant differences were found in baseline scores among the groups (**Fig. 8a**). As expected, scores were sharply reduced in all groups at 1 wpi. At 2 wpi, the control and PF groups performed poorly, and the RO48-treated groups appeared to have improved performance in comparison; for the 4mM group, this difference reached statistical significance (**Fig. 8a**). By 4 wpi, and continuing to 8 wpi, both RO48 treatments significantly increased fall latency compared to DMSO and PF groups (**Fig. 8a**). The 30mM RO48 treatment group showed increased latencies at each of these times compared to the 4mM RO48 treatment, and at 8 wpi this difference was statistically significant, suggesting a dose-response relationship for this outcome measure.

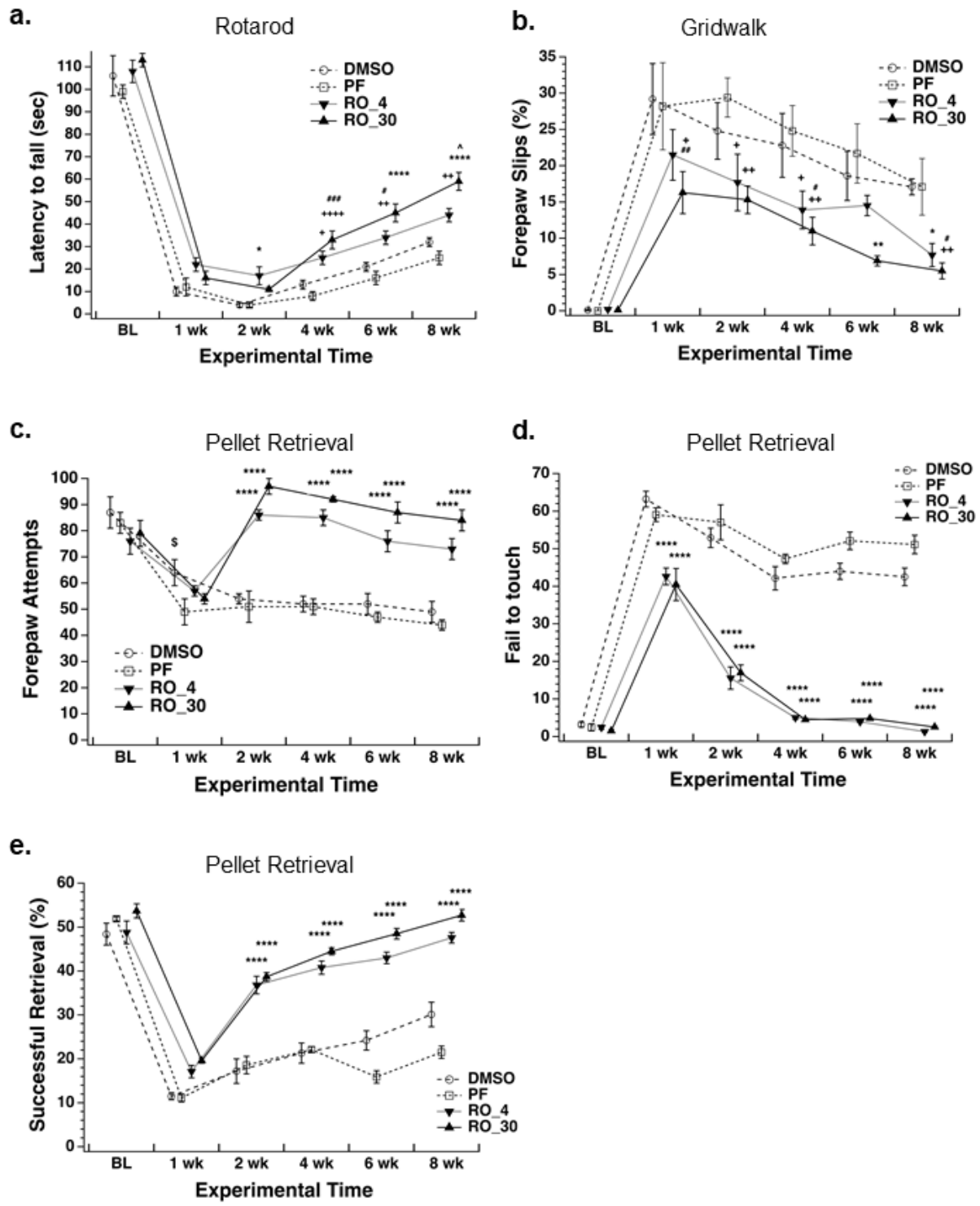

Figure 8. RO48 injected into the motor cortex promotes behavioral recovery after a C5 dorsal hemisection. a) Rotarod fall latency is plotted for DMSO control (open circles), PF (open squares), 4 mM RO48 (RO_4, downward triangles) and 30 mM RO48 (RO_30, upward triangles). All groups rapidly fell off when tested at 1 wpi. More rapid improvement was seen in

the two RO48 groups compared to DMSO and PF, and these differences reached statistical significance starting at 2 wpi. b) Number of forepaw slips below the grid in gridwalk test. Slips increased variably by 1 wpi. Although improvements were seen in control and PF groups over 8 wpi, improvements were significantly more rapid and extensive in the two RO48 groups. c-e) Results from pellet retrieval test. c) Animals made significantly more attempts in the two RO48 groups by 2 wpi, continuing through 8 wpi. d) Both RO48 groups showed substantial declines in the % of touch failures over 8 wpi, reaching levels close to baseline by the end. In contrast, control and PF groups did not improve substantially over 8 wpi. e) After training, each group reached retrieval success rates close to 50%; these rates fell substantially 1 wpi. Compared to control and PF groups, both RO48 groups improved significantly starting at 2 wpi, and by 8 wpi attained success rates comparable to pre-injury baseline. Symbols for data of the different groups collected at the same time point are offset on the x axis for clearer visualization. Data are expressed as mean ± SEM ,n=8, DMSO; n=5, PF; n=8, RO_4; n=6, RO_30. ****$p < 0.0001$, **$p < 0.01$, *$p < 0.05$, RO_4, RO_30 vs PF and DMSO; ++++$p < 0.0001$, ++$p < 0.01$, +$p < 0.05$, RO_4, RO_30 vs PF; ###$p < 0.001$, ##$p < 0.01$, #$p < 0.05$, RO_4, RO_30 vs DMSO; ^$p < 0.05$, RO_4 vs RO_30; \$$p < 0.05$, PF vs DMSO.

In the gridwalk test, we again measured forepaw drops below the level of the grid. After pretraining, baseline errors were rare (< 0.1%), and no differences were observed among groups (**Fig. 8b**). At 1wpi, control animals (and PF-treated animals) showed error rates > 25%, while rates for both RO48 groups were lower, though not significantly different for the 4mM group. This trend continued at 4,6, and 8 wpi, with both RO48 treatment groups making significantly fewer errors than controls or PF-treated animals (with the exception of the 4mM group at 6 wpi). Although there were no significant differences between the two RO48 treatments, the 30mM group consistently exhibited better scores than the 4mM group at each time point starting at 2 wpi (**Fig. 8b**).

In the single-pellet retrieval test, mice were pretrained for 16 days, including food deprivation, shaping, and training stages (Al-Ali et al., 2017; Chen et al., 2014). We measured several aspects of this task, including total attempts, touching of the pellet, and successful retrievals. Total forepaw attempts are plotted in **Fig. 8c**, and failures to touch the pellet (**Fig. 8d**) and successful retrievals (**Fig. 8e**) are plotted as percentages of total attempts. At 1 wpi, total forepaw attempts in all groups were markedly reduced, and their frequency did not recover detectably in control or PF-treated groups over 8 wpi. However, both RO48 treatments significantly increased forepaw attempts at 4, 6, and 8 wpi as compared to both PF and control groups (**Fig. 8c**). RO48-treated animals were also more successful in their attempts. DMSO and PF-treated groups failed to touch the pellet nearly 50% of the time after the injury. Starting from 1 wpi, however, both RO48 treatment groups showed decreased touch failure rates compared to PF and control, returning to near baseline rates by 8 wpi (**Fig. 8d)**. Both doses of RO48 also significantly increased successful pellet retrieval rates at 2-8 wpi compared to both PF and control groups (**Fig. 8e**). Strikingly, retrieval rate (the criterion for success in this test) in the two RO48 groups returned essentially to baseline levels at 8 wpi. There was no clear evidence of a dose-response relationship for RO48 in this outcome measure, suggesting that both concentrations may be near a plateau level for this test. Overall, we confirmed that RO48, when delivered to sensorimotor cortex, improved forelimb motor function after a C5 dorsal hemisection injury.

These *in vivo* experiments, taken together, show that microinjection of RO48 into sensorimotor cortex promoted sprouting and regeneration of CST axons in several different injury models, improved behavioral outcomes after dorsal hemisection in two separate experimental series, and, in our hands, showed better efficacy compared to two other treatments previously shown to be effective in SCI models (Y27632 and PF-4708671). This provides strong evidence for the robustness of RO48's growth-promoting ability for CST axons, and suggests that this compound improves functional recovery in some injury settings.

Discussion

Axon regeneration in the CNS is impaired both by a lack of intrinsic regenerative capacity in CNS neurons and by numerous inhibitory factors in the injury microenvironment. We approached this challenge by identifying kinases whose inhibition leads to neurite outgrowth promotion in primary CNS neurons, including ROCK1/2 (involved in extrinsic axon growth repression), S6K1 (involved in intrinsic regenerative signaling; Al-Ali et al., 2017), and others (Al-Ali et al., 2015). Examination of compound polypharmacology profiles revealed that the KI with the highest activity in our neurite outgrowth assay, RO48, co-inhibited S6K1 and ROCK1/2, in addition to PKX, PKG1, and PKCγ. We now show that RO48 promotes neurite outgrowth in a variety of mammalian CNS neurons, including postnatal cortical neurons, adult sensory neurons, and human iPSC-derived glutamatergic neurons. These results increase confidence that targeting multiple kinases with a single compound is a useful strategy for increasing axon growth.

In accord with this idea, the current studies show that a single injection of RO48 into sensorimotor cortex can induce CST axon growth in three different injury models--pyramidotomy, funiculotomy, and dorsal hemisection. Notably, RO48 treatment following dorsal hemisection also resulted in improvements in distinct functional outcome measures. These results suggest that cortical treatment with RO48 helps to rewire the neural network controlling forelimb movements, presumably as a result of selective increases in axon growth in the spinal cord and/or brain. Because some of the functional improvements associated with RO48 administration were evident as early as 1-2 wpi, and because CST regeneration past the lesion was not long distance or highly profuse even at later times, it is not likely that all observed functional improvements can be linked to CST regeneration past the lesion. Potential changes associated with improved recovery could include CST growth into or compensatory sprouting in other motor control regions (Nicola et al., 2022), such as the rubrospinal tract (Morris et al., 2011), the cerebellothalamic tracts (Sakayori et al., 2019), and/or the medullary reticular formation (Esposito et al., 2014). RO48 could also be involved in re-wiring of spinal cord circuits, and/or growth of additional supraspinal axons (such as serotonergic projections); we did not examine these possibilities. Further improvements in motor control could be potentiated by combining RO48 treatment with rehabilitative training, a widely used treatment strategy that has been shown to improve outcomes in SCI patients (Alcobendas-Maestro et al., 2012; Harkema et al., 2012; Kapadia et al., 2013; Nam et al., 2017).

In the pyramidotomy model, increases in contralateral sprouting with experimental interventions are normally thought to be triggered by the presence of denervated projection zones/synaptic targets in the gray matter. Our results with RO48 contrast with this view; RO48 increased CST axon sprouting in the cervical cord in uninjured animals, or when administered 8 weeks after an injury. These data indicate that RO48 does not promote axon growth solely in response to an acute injury signal, suggesting that RO48 could promote growth in chronic or sub-acute spinal cord injury conditions that are more typical of therapeutic opportunities in SCI. Increased axonal sprouting in uninjured tissue can be seen as a perturbation to an otherwise normal and

homeostatic neuronal circuit. While it is tempting to assume that these changes in circuitry would have negative consequences for the experimental animals, there were no obvious differences in behavior and/or motor control between the groups in these experiments.

Kinases mediate both CNS degenerative and regenerative processes (Al-Ali et al., 2016, 2015; Chico et al., 2009; Krahn et al., 2020). Additionally, KIs are amenable to systematic approaches that wield polypharmacology by design (Al-Ali et al., 2015; Klaeger et al., 2017). Although once believed to be inherently toxic, the clinical safety profiles of KIs have improved, and they are undergoing clinical development for numerous non-oncology indications ranging from metabolic disorders to immunology, inflammation, and even infectious diseases, including COVID-19 (Ferguson and Gray, 2018; Kalil et al., 2020; Klaeger et al., 2017; Knight et al., 2010; Mueller et al., 2005; Wang et al., 2014; Zhang et al., 2009). A phase 2b/3 clinical trial evaluating masitinib in patients with Alzheimer's recently met its primary endpoint, underscoring the large untapped potential for kinase inhibitors as drugs for neurological disorders.

There are still no approved drugs for promoting axon regeneration, though a number of therapeutic candidates have entered clinical trials. This includes candidates that target components of the extrinsic inhibitory pathway characterized by activation of RhoA/ROCK (Duffy et al., 2009; Gopalakrishnan et al., 2008; Lingor et al., 2007; Monnier et al., 2003; Young, 2014), and other candidates targeting extrinsic inhibitory mechanisms, including GlaxoSmithKline's GSK249320A, Novartis's ATI355, and ReNetX Bio's AXER-204, each of which targets inhibition through myelin-associated proteins. So far, no successful Phase II/III studies have been reported for these candidates. Therapeutic candidates that target intrinsic regenerative mechanisms have also been investigated. This category includes protein biologics such as Kringle Pharma's KP-100IT (an engineered dimeric fragment of human hepatocyte growth factor) and BioArctic AB's SC0806 (a biodegradable implant that delivers Fibroblast Growth Factor 1). So far, no positive efficacy data have been reported for these candidates. Additionally, cell therapy-based clinical trials are being conducted with a variety of cell types (Assinck et al., 2017); some have shown initial promise but none has demonstrated clinical efficacy to date. This history suggests that new therapeutic approaches, such as that exemplified by RO48, may be valuable.

Conclusions

It is commonly reported that preclinical target discovery and animal model validation studies have major issues relating to robustness and reproducibility (Begley and Ellis, 2012; Frye et al., 2015; Nosek and Errington, 2017; Prinz et al., 2011), and this is no less true for neuroscience (Bernard, 2020; Button et al., 2013; Watzlawick et al., 2019). This situation has been analyzed in a variety of studies (Button et al., 2013; Ulrich and Miller, 2020; Watzlawick et al., 2019; Witt, 2019). Although some reproducibility issues are difficult to avoid, we have employed a variety of strategies and tactics to increase the chances that our approach and experimental results are valid. First, a low "base rate", or the odds of success prior to beginning an experiment, has a large influence on the likelihood of true positive effects (Ulrich and Miller, 2020). An important way we have tried to increase prior odds lies in our use of polypharmacology, and in an experimental compound that targets both intrinsic and extrinsic pathways of axon growth inhibition. With respect to experimental design, we used blinding of experimenters as well as random block allocation methods for the groups in our animal studies. In our animal studies, we used three different experimental models, and multiple experimental series taking advantage of multiple surgeons, completing experimental series in three different laboratories in two distinct locations (Indiana and Miami) to validate *in vivo* effects of RO48. We have reported results from each of our experimental series, in an effort to be transparent. Some of these results differ in

detail from one another, but the overall pattern allows the conclusion that RO48 can promote axon growth *in vivo*. Given that RO48 is also active on human neurons, it seems worthwhile to pursue studies that aim to translate these results into efforts to develop novel therapeutics for human spinal cord injury.

Acknowledgments

This work was supported by grants from the NIH (R01NS100531, VPL and JLB; R41TR002293, HA; R01NS103481, R01NS111776, XMX), the Indiana Department of Health's Indiana Spinal Cord and Brain Injury Research Grant (ISDH58180, WW), the UM Wallace H Coulter Center (HA, VPL, and JLB), the State of Florida (HA), and the Miami Project to Cure Paralysis. VPL holds the Walter G. Ross Distinguished Chair of Developmental Neuroscience. The funding sources had no involvement in collection, analysis, or interpretation of data; nor in writing or decision to submit for publication. We thank Phil Popovich, Jae Lee and Nicholas O'Neill for helpful discussions, and Abdiel Badillo, Yania Martinez, and Tania Slepak for outstanding technical assistance. We thank Yan Shi in the Miami Project Imaging Core and Yania Martinez in the Miami Project Viral Vector Core for invaluable services. We would also like to acknowledge Bascom Palmer Eye Institute's NIH Center Core Grant P30EY014801 and Research to Prevent Blindness' Unrestricted Grant (GR004596) for the use of their Imaging Core.

References

Al-Ali, H., 2016. The evolution of drug discovery: From phenotypes to targets, and back. Medchemcomm 7, 788–798. https://doi.org/10.1039/c6md00129g

Al-Ali, H., Bixby, J.L., Lemmon, V.P., 2016. Exploiting kinase polypharmacology for nerve regeneration. Neural Regen. Res. 11, 71–72. https://doi.org/10.4103/1673-5374.169614

Al-Ali, H., Blackmore, M., Bixby, J.L., Lemmon, V.P., 2004. High Content Screening with Primary Neurons. Assay Guid. Man.

Al-Ali, H., Ding, Y., Slepak, T., Wu, W., Sun, Y., Martinez, Y., Xu, X.M., Lemmon, V.P., Bixby, J.L., 2017. The mTOR substrate S6 kinase 1 (S6K1) is a negative regulator of axon regeneration and a potential drug target for central nervous system injury. J. Neurosci. 37, 7079–7095. https://doi.org/10.1523/JNEUROSCI.0931-17.2017

Al-Ali, H., Lee, D.H., Danzi, M.C., Nassif, H., Gautam, P., Wennerberg, K., Zuercher, B., Drewry, D.H., Lee, J.K., Lemmon, V.P., Bixby, J.L., 2015. Rational Polypharmacology: Systematically Identifying and Engaging Multiple Drug Targets to Promote Axon Growth. ACS Chem. Biol. 10, 1939–1951. https://doi.org/10.1021/acschembio.5b00289

Al-Ali, H., Schürer, S.C., Lemmon, V.P., Bixby, J.L., 2013. Chemical interrogation of the neuronal kinome using a primary cell-based screening assay. ACS Chem. Biol. 8, 1027–36. https://doi.org/10.1021/cb300584e

Alcobendas-Maestro, M., Esclarín-Ruz, A., Casado-López, R.M., Muñoz-González, A., Pérez-Mateos, G., González-Valdizán, E., Martín, J.L.R., 2012. Lokomat robotic-assisted versus overground training within 3 to 6 months of incomplete spinal cord lesion: randomized controlled trial. Neurorehabil. Neural Repair 26, 1058–1063. https://doi.org/10.1177/1545968312448232

Anderson, K.D., Gunawan, A., Steward, O., 2005. Quantitative assessment of forelimb motor function after cervical spinal cord injury in rats: relationship to the corticospinal tract. Exp. Neurol. 194, 161–174. https://doi.org/10.1016/j.expneurol.2005.02.006

Assinck, P., Duncan, G.J., Hilton, B.J., Plemel, J.R., Tetzlaff, W., 2017. Cell transplantation therapy for spinal cord injury. Nat. Neurosci. https://doi.org/10.1038/nn.4541

Beckerman, S.R., Jimenez, J.E., Shi, Y., Al-Ali, H., Bixby, J.L., Lemmon, V.P., 2015. Phenotypic Assays to Identify Agents That Induce Reactive Gliosis: A Counter-Screen to Prioritize Compounds for Preclinical Animal Studies. Assay Drug Dev. Technol. 13, 377–388. https://doi.org/10.1089/adt.2015.654

Begley, C.G., Ellis, L.M., 2012. Drug development: Raise standards for preclinical cancer research. Nature 483, 531–3. https://doi.org/10.1038/483531a

Bernard, C., 2020. On fallacies in neuroscience. eNeuro. https://doi.org/10.1523/ENEURO.0491-20.2020

Button, K.S., Ioannidis, J.P.A., Mokrysz, C., Nosek, B.A., Flint, J., Robinson, E.S.J., Munafò, M.R., 2013. Power failure: Why small sample size undermines the reliability of neuroscience. Nat. Rev. Neurosci. 14, 365–376. https://doi.org/10.1038/nrn3475

Chan, C.C.M., Khodarahmi, K., Liu, J., Sutherland, D., Oschipok, L.W., Steeves, J.D., Tetzlaff, W., 2005. Dose-dependent beneficial and detrimental effects of ROCK inhibitor Y27632 on axonal sprouting and functional recovery after rat spinal cord injury. Exp. Neurol. 196, 352–364. https://doi.org/10.1016/j.expneurol.2005.08.011

Chico, L.K., Van Eldik, L.J., Watterson, D.M., 2009. Targeting protein kinases in central nervous

system disorders. Nat. Rev. Drug Discov. https://doi.org/10.1038/nrd2999

Cohen, P., 2002. Protein kinases - The major drug targets of the twenty-first century? Nat. Rev. Drug Discov. 1, 309–315. https://doi.org/10.1038/nrd773

Duffy, P., Schmandke, Andre, Schmandke, Antonio, Sigworth, J., Narumiya, S., Cafferty, W.B.J., Strittmatter, S.M., 2009. Rho-associated kinase II (ROCKII) limits axonal growth after trauma within the adult mouse spinal cord. J. Neurosci. 29, 15266–76. https://doi.org/10.1523/JNEUROSCI.4650-09.2009

Eder, J., Sedrani, R., Wiesmann, C., 2014. The discovery of first-in-class drugs: Origins and evolution. Nat. Rev. Drug Discov. 13, 577–587. https://doi.org/10.1038/nrd4336

Esposito, M.S., Capelli, P., Arber, S., 2014. Brainstem nucleus MdV mediates skilled forelimb motor tasks. Nature 508, 351–356. https://doi.org/10.1038/nature13023

Ferguson, F.M., Gray, N.S., 2018. Kinase inhibitors: the road ahead. Nat. Rev. Drug Discov. 17, 353–377. https://doi.org/10.1038/nrd.2018.21

Forgione, N., Chamankhah, M., Fehlings, M.G., 2017. A Mouse Model of Bilateral Cervical Contusion-Compression Spinal Cord Injury. J. Neurotrauma 34, 1227–1239. https://doi.org/10.1089/neu.2016.4708

Fournier, A.E., Takizawa, B.T., Strittmatter, S.M., 2003. Rho kinase inhibition enhances axonal regeneration in the injured CNS. J. Neurosci. 23, 1416–23. https://doi.org/10.1523/jneurosci.23-04-01416.2003

Frye, S. V., Arkin, M.R., Arrowsmith, C.H., Conn, P.J., Glicksman, M.A., Hull-Ryde, E.A., Slusher, B.S., 2015. Tackling reproducibility in academic preclinical drug discovery. Nat. Rev. Drug Discov. https://doi.org/10.1038/nrd4737

Gautam, P., Jaiswal, A., Aittokallio, T., Al-Ali, H., Wennerberg, K., 2019. Phenotypic Screening Combined with Machine Learning for Efficient Identification of Breast Cancer-Selective Therapeutic Targets. Cell Chem. Biol. 26, 970-979.e4. https://doi.org/10.1016/J.CHEMBIOL.2019.03.011

Gopalakrishnan, S.M., Teusch, N., Imhof, C., Bakker, M.H.M., Schurdak, M., Burns, D.J., Warrior, U., 2008. Role of Rho kinase pathway in chondroitin sulfate proteoglycan-mediated inhibition of neurite outgrowth in PC12 cells. J. Neurosci. Res. 86, 2214–26. https://doi.org/10.1002/jnr.21671

Gray, J.A., Roth, B.L., 2006. Developing selectively nonselective drugs for treating CNS disorders. Drug Discov. Today Ther. Strateg. 3, 413–419. https://doi.org/10.1016/j.ddstr.2006.11.009

Harkema, S.J., Schmidt-Read, M., Lorenz, D.J., Edgerton, V.R., Behrman, A.L., 2012. Balance and ambulation improvements in individuals with chronic incomplete spinal cord injury using locomotor training-based rehabilitation. Arch. Phys. Med. Rehabil. 93, 1508–1517. https://doi.org/10.1016/j.apmr.2011.01.024

Huebner, E.A., Strittmatter, S.M., 2009. Axon regeneration in the peripheral and central nervous systems. Results Probl. Cell Differ., Results and Problems in Cell Differentiation 48, 339–351. https://doi.org/10.1007/400_2009_19

Ichikawa, M., Yoshida, J., Saito, K., Sagawa, H., Tokita, Y., Watanabe, M., 2008. Differential effects of two ROCK inhibitors, Fasudil and Y-27632, on optic nerve regeneration in adult cats. Brain Res. 1201, 23–33. https://doi.org/10.1016/j.brainres.2008.01.063

Kalil, A.C., Patterson, T.F., Mehta, A.K., Tomashek, K.M., Wolfe, C.R., Ghazaryan, V., Marconi,

V.C., Ruiz-Palacios, G.M., Hsieh, L., Kline, S., Tapson, V., Iovine, N.M., Jain, M.K., Sweeney, D.A., El Sahly, H.M., Branche, A.R., Regalado Pineda, J., Lye, D.C., Sandkovsky, U., Luetkemeyer, A.F., Cohen, S.H., Finberg, R.W., Jackson, P.E.H., Taiwo, B., Paules, C.I., Arguinchona, H., Erdmann, N., Ahuja, N., Frank, M., Oh, M., Kim, E.-S., Tan, S.Y., Mularski, R.A., Nielsen, H., Ponce, P.O., Taylor, B.S., Larson, L., Rouphael, N.G., Saklawi, Y., Cantos, V.D., Ko, E.R., Engemann, J.J., Amin, A.N., Watanabe, M., Billings, J., Elie, M.-C., Davey, R.T., Burgess, T.H., Ferreira, J., Green, M., Makowski, M., Cardoso, A., de Bono, S., Bonnett, T., Proschan, M., Deye, G.A., Dempsey, W., Nayak, S.U., Dodd, L.E., Beigel, J.H., 2020. Baricitinib plus Remdesivir for Hospitalized Adults with Covid-19. N. Engl. J. Med. NEJMoa2031994. https://doi.org/10.1056/nejmoa2031994

Kapadia, N., Zivanovic, V., Popovic, M.R., 2013. Restoring voluntary grasping function in individuals with incomplete chronic spinal cord injury: pilot study. Top. Spinal Cord Inj. Rehabil. 19, 279–287. https://doi.org/10.1310/sci1904-279

Klaeger, S., Heinzlmeir, S., Wilhelm, M., Polzer, H., Vick, B., Koenig, P.-A., Reinecke, M., Ruprecht, B., Petzoldt, S., Meng, C., Zecha, J., Reiter, K., Qiao, H., Helm, D., Koch, H., Schoof, M., Canevari, G., Casale, E., Depaolini, S.R., Feuchtinger, A., Wu, Z., Schmidt, T., Rueckert, L., Becker, W., Huenges, J., Garz, A.-K., Gohlke, B.-O., Zolg, D.P., Kayser, G., Vooder, T., Preissner, R., Hahne, H., Tõnisson, N., Kramer, K., Götze, K., Bassermann, F., Schlegl, J., Ehrlich, H.-C., Aiche, S., Walch, A., Greif, P.A., Schneider, S., Felder, E.R., Ruland, J., Médard, G., Jeremias, I., Spiekermann, K., Kuster, B., 2017. The target landscape of clinical kinase drugs. Science (80-.). 358, eaan4368. https://doi.org/10.1126/SCIENCE.AAN4368

Knight, Z.A., Lin, H., Shokat, K.M., 2010. Targeting the cancer kinome through polypharmacology. Nat. Rev. Cancer 10, 130–137. https://doi.org/10.1038/nrc2787

Krahn, A.I., Wells, C., Drewry, D.H., Beitel, L.K., Durcan, T.M., Axtman, A.D., 2020. Defining the Neural Kinome: Strategies and Opportunities for Small Molecule Drug Discovery to Target Neurodegenerative Diseases. ACS Chem. Neurosci. 11, 1871–1886. https://doi.org/10.1021/acschemneuro.0c00176

Lee, D.H., Luo, X.T., Yungher, B.J., Bray, E., Lee, J.K., Park, K.K., 2014. Mammalian Target of Rapamycin's Distinct Roles and Effectiveness in Promoting Compensatory Axonal Sprouting in the Injured CNS. J. Neurosci. 34, 15347–15355. https://doi.org/10.1523/jneurosci.1935-14.2014

Lerch, J.K., Alexander, J.K., Madalena, K.M., Motti, D., Quach, T., Dhamija, A., Zha, A., Gensel, J.C., Marketon, J.W., Lemmon, V.P., Bixby, J.L., Popovich, P.G., 2017. Stress increases peripheral axon growth and regeneration through glucocorticoid receptor-dependent transcriptional programs. eNeuro 4. https://doi.org/10.1523/ENEURO.0246-17.2017

Lingor, P., Teusch, N., Schwarz, K., Mueller, R., Mack, H., Bähr, M., Mueller, B.K., 2007. Inhibition of Rho kinase (ROCK) increases neurite outgrowth on chondroitin sulphate proteoglycan in vitro and axonal regeneration in the adult optic nerve in vivo. J. Neurochem. 103, 181–9. https://doi.org/10.1111/j.1471-4159.2007.04756.x

Lingor, P., Tönges, L., Pieper, N., Bermel, C., Barski, E., Planchamp, V., Bähr, M., 2008. ROCK inhibition and CNTF interact on intrinsic signalling pathways and differentially regulate survival and regeneration in retinal ganglion cells. Brain 131, 250–263. https://doi.org/10.1093/brain/awm284

Liu, N.K., Zhang, Y.P., O'Connor, J., Gianaris, A., Oakes, E., Lu, Q.B., Verhovshek, T., Walker, C.L., Shields, C.B., Xu, X.M., 2013. A bilateral head injury that shows graded brain damage

and behavioral deficits in adultmice. Brain Res. 1499, 121–128. https://doi.org/10.1016/j.brainres.2012.12.031

Mestres, J., Gregori-Puigjané, E., Valverde, S., Solé, R. V, 2009. The topology of drug-target interaction networks: implicit dependence on drug properties and target families. Mol. Biosyst. 5, 1051–7. https://doi.org/10.1039/b905821b

Metz, J.T., Hajduk, P.J., 2010. Rational approaches to targeted polypharmacology: creating and navigating protein-ligand interaction networks. Curr. Opin. Chem. Biol. 14, 498–504. https://doi.org/10.1016/j.cbpa.2010.06.166

Monnier, P.P., Sierra, A., Schwab, J.M., Henke-Fahle, S., Mueller, B.K., 2003. The Rho/ROCK pathway mediates neurite growth-inhibitory activity associated with the chondroitin sulfate proteoglycans of the CNS glial scar. Mol. Cell. Neurosci. 22, 319–330. https://doi.org/10.1016/S1044-7431(02)00035-0

Morris, R., Tosolini, A.P., Goldstein, J.D., Whishaw, I.Q., 2011. Impaired Arpeggio Movement in Skilled Reaching by Rubrospinal Tract Lesions in the Rat: A Behavioral/Anatomical Fractionation. J. Neurotrauma 28, 2439–2451. https://doi.org/10.1089/neu.2010.1708

Mueller, B.K., Mack, H., Teusch, N., 2005. Rho kinase, a promising drug target for neurological disorders. Nat. Rev. Drug Discov. 4, 387–98. https://doi.org/10.1038/nrd1719

Nam, K.Y., Kim, H.J., Kwon, B.S., Park, J.-W., Lee, H.J., Yoo, A., 2017. Robot-assisted gait training (Lokomat) improves walking function and activity in people with spinal cord injury: a systematic review. J. Neuroeng. Rehabil. 14, 24. https://doi.org/10.1186/s12984-017-0232-3

Nicola, F. do C., Hua, I., Levine, A.J., 2022. Intersectional genetic tools to study skilled reaching in mice. Exp. Neurol. 347, 113879. https://doi.org/10.1016/J.EXPNEUROL.2021.113879

Nosek, B.A., Errington, T.M., 2017. Making sense of replications. Elife 6. https://doi.org/10.7554/eLife.23383

Patel, A.K., Broyer, R.M., Lee, C.D., Lu, T., Louie, M.J., La Torre, A., Al-Ali, H., Vu, M.T., Mitchell, K.L., Wahlin, K.J., Berlinicke, C.A., Jaskula-Ranga, V., Hu, Y., Duan, X., Vilar, S., Bixby, J.L., Weinreb, R.N., Lemmon, V.P., Zack, D.J., Welsbie, D.S., 2020. Inhibition of GCK-IV kinases dissociates cell death and axon regeneration in CNS neurons. Proc. Natl. Acad. Sci. 117, 33597–33607. https://doi.org/10.1073/pnas.2004683117

Peters, J.-U., 2013. Polypharmacology - foe or friend? J. Med. Chem. 56, 8955–71. https://doi.org/10.1021/jm400856t

Petrelli, A., 2012. Polypharmacological Kinase Inhibitors: New Hopes for Cancer Therapy. Polypharmacology Drug Discov. 149–165. https://doi.org/10.1002/9781118098141.ch8

Prinz, F., Schlange, T., Asadullah, K., 2011. Believe it or not: how much can we rely on published data on potential drug targets? Nat. Rev. Drug Discov. 10, 712. https://doi.org/10.1038/nrd3439-c1

Sakayori, N., Kato, S., Sugawara, M., Setogawa, S., Fukushima, H., Ishikawa, R., Kida, S., Kobayashi, K., 2019. Motor skills mediated through cerebellothalamic tracts projecting to the central lateral nucleus. Mol. Brain 12, 1–12. https://doi.org/10.1186/S13041-019-0431-X/FIGURES/4

Schindelin, J., Arganda-Carreras, I., Frise, E., Kaynig, V., Longair, M., Pietzsch, T., Preibisch, S., Rueden, C., Saalfeld, S., Schmid, B., Tinevez, J.Y., White, D.J., Hartenstein, V., Eliceiri, K., Tomancak, P., Cardona, A., 2012. Fiji: An open-source platform for biological-image

analysis. Nat. Methods. https://doi.org/10.1038/nmeth.2019

Schrimsher, G.W., Reier, P.J., 1992. Forelimb motor performance following cervical spinal cord contusion injury in the rat. Exp. Neurol. 117, 287–298. https://doi.org/10.1016/0014-4886(92)90138-G

Steward, O., Popovich, P.G., Dietrich, W.D., Kleitman, N., 2012. Replication and reproducibility in spinal cord injury research. Exp. Neurol. 233, 597–605. https://doi.org/10.1016/j.expneurol.2011.06.017

Streijger, F., Beernink, T.M.J., Lee, J.H.T., Bhatnagar, T., Park, S., Kwon, B.K., Tetzlaff, W., 2013. Characterization of a cervical spinal cord hemicontusion injury in mice using the infinite horizon impactor. J. Neurotrauma 30, 869–883. https://doi.org/10.1089/neu.2012.2405

Swinney, D.C., 2013. Phenotypic vs. Target-based drug discovery for first-in-class medicines. Clin. Pharmacol. Ther. 93, 299–301. https://doi.org/10.1038/clpt.2012.236

Swinney, D.C., Anthony, J., 2011. How were new medicines discovered? Nat. Rev. Drug Discov. 10, 507–19. https://doi.org/10.1038/nrd3480

Ulrich, R., Miller, J., 2020. Meta-research: Questionable research practices may have little effect on replicability. Elife 9, 1–74. https://doi.org/10.7554/ELIFE.58237

Vincent, F., Loria, P.M., Weston, A.D., Steppan, C.M., Doyonnas, R., Wang, Y.M., Rockwell, K.L., Peakman, M.C., 2020. Hit Triage and Validation in Phenotypic Screening: Considerations and Strategies. Cell Chem. Biol. 27, 1332–1346. https://doi.org/10.1016/j.chembiol.2020.08.009

Walker, C.L., Fry, C.M.E., Wang, J., Du, X., Zuzzio, K., Liu, N.K., Walker, M.J., Xu, X.M., 2019. Functional and Histological Gender Comparison of Age-Matched Rats after Moderate Thoracic Contusive Spinal Cord Injury. J. Neurotrauma 36, 1974–1984. https://doi.org/10.1089/neu.2018.6233

Wang, X., Hu, J., She, Y., Smith, G.M., Xu, X.M., 2014. Cortical PKC inhibition promotes axonal regeneration of the corticospinal tract and forelimb functional recovery after cervical dorsal spinal hemisection in adult rats. Cereb. Cortex 24, 3069–3079. https://doi.org/10.1093/cercor/bht162

Wang, Z., Reynolds, A., Kirry, A., Nienhaus, C., Blackmore, M.G., 2015. Overexpression of Sox11 promotes corticospinal tract regeneration after spinal injury while interfering with functional recovery. J. Neurosci. 35, 3139–3145. https://doi.org/10.1523/JNEUROSCI.2832-14.2015

Watzlawick, R., Antonic, A., Sena, E.S., Kopp, M.A., Rind, J., Dirnagl, U., Macleod, M., Howells, D.W., Schwab, J.M., 2019. Outcome heterogeneity and bias in acute experimental spinal cord injury: A meta-analysis. Neurology 93, E40–E51. https://doi.org/10.1212/WNL.0000000000007718

Witt, J.K., 2019. Insights into Criteria for Statistical Significance from Signal Detection Analysis. Meta-Psychology 3. https://doi.org/10.15626/mp.2018.871

Wu, W., Xiong, W., Zhang, P., Chen, L., Fang, J., Shields, C., Xu, X.M., Jin, X., 2017. Increased threshold of short-latency motor evoked potentials in transgenic mice expressing Channelrhodopsin-2. PLoS One 12. https://doi.org/10.1371/journal.pone.0178803

Young, W., 2014. Spinal cord regeneration. Cell Transplant. 23, 573–611. https://doi.org/10.3727/096368914X678427

Zhang, J., Yang, P.L., Gray, N.S., 2009. Targeting cancer with small molecule kinase inhibitors. Nat. Rev. Cancer 9, 28–39. https://doi.org/10.1038/nrc2559

Zhang, Y.P., Walker, M.J., Shields, L.B.E., Wang, X., Walker, C.L., Xu, X.-M., Shields, C.B., 2013. Controlled Cervical Laceration Injury in Mice. J. Vis. Exp. e50030. https://doi.org/10.3791/50030

Declaration of interest

HAA, VPL, and JLB are inventors on an international patent application filed by the University of Miami to cover the compounds described in this study (No. PCT/US18/58411).

Mah et al., EXNR-22-233, Highlights

- Kinase inhibitor RO48 targets both intrinsic and extrinsic axon-inhibitory pathways
- RO48 promotes neurite outgrowth in multiple neuronal types, including human neurons
- RO48 promotes corticospinal axon growth in injury models when delivered to cortex
- Axon growth induced by RO48 does not require an acute injury
- Results from distinct laboratories suggest that in vivo effects of RO48 are robust